

doi: 10.3978/j.issn.2095-6959.2022.05.011

View this article at: <https://dx.doi.org/10.3978/j.issn.2095-6959.2022.05.011>

基于计算机断层扫描阈值分割评估儿童 法洛四联症心功能的临床应用价值

应波¹, 徐佳俊², 钱红萍¹

(1. 桐庐县妇幼保健院儿科, 浙江 桐庐 311500; 2. 浙江大学医学院附属儿童医院心脏监护病房, 杭州 310052)

[摘要] 目的: 研究计算机断层扫描(computed tomography, CT)阈值分割评估儿童法洛四联症(tetralogy of Fallot, TOF)心功能的可行性及其临床应用价值。方法: 回顾性纳入2018年11月至2019年12月诊断为TOF并行手术治疗的患儿38例, 术前、术后6个月随访时行计算机断层扫描血管造影术(computed tomography angiography, CTA)扫描, 获取图像, 通过阈值分割法评估左、右心功能参数, 包括左、右心室舒张末期容积、收缩末期容积、每搏输出量及射血分数。对比分析TOF患儿术前与术后6个月左、右心室容积和心功能参数变化, 并进行统计分析。结果: CT基于阈值分割可同时评估TOF患儿左、右心功能参数。术后6个月与术前相比, 左心功能参数无明显变化, 差异无统计学意义, 术后右心室收缩末期容积略高于术前[(23.88±7.44) mL/m² vs (19.67±6.52) mL/m²], 但差异无统计学意义(P=0.066), 术后右心室舒张末期容积略高于术前[(49.86±14.82) mL/m² vs (46.30±14.46) mL/m²], 但差异无统计学意义(P=0.079); 术后右心射血分数低于术前(51.47%±4.68% vs 57.84%±5.09%), 差异有统计学意义(P=0.001)。结论: 基于CT阈值分割可准确评估TOF患儿左、右心功能, 可以早期发现术后右心功能下降, 从而及时采取干预措施, 对TOF患儿预后评估有重要意义。

[关键词] 计算机断层扫描; 法洛四联症; 心功能; 阈值分割

Clinical value of computed tomography based on volume rendering in assessment of cardiac function in children with tetralogy of Fallot

YING Bo¹, XU Jiajun², QIAN Hongping¹

(1. Department of Pediatrics, Tonglu Maternal and Child Health Hospital, Tonglu Zhejiang 311500; 2. Department of Cardiac Intensive Care Unit, Children's Hospital, Zhejiang University School of Medicine, Hangzhou 310052, China)

Abstract **Objective:** To investigate the clinical value of computed tomography (CT) based on volume rendering in evaluating cardiac function in children with tetralogy of Fallot. **Methods:** Thirty-eight children with tetralogy

收稿日期 (Date of reception): 2021-04-25

通信作者 (Corresponding author): 应波, Email: 529674111@qq.com

基金项目 (Foundation item): 桐庐县科技局计划项目 (2019 第 28 号)。This work was supported by the Project of Tonglu County Science and Technology Bureau, Zhejiang Province, China [(2019) No. 28].

of Fallot in our hospital from November 2018 to December 2019 were retrospectively enrolled in this study. CT scanning were performed before and 6 months after surgery. CT images were acquired and segmented by volume rendering to evaluate left and right ventricular function parameters including left and right ventricular end-diastolic volume, end-systolic volume, stroke volume, and ejection fraction. The left and right ventricular volume and cardiac function parameter changes of children with tetralogy of Fallot preoperatively and 6 months after operation were statistically compared. **Results:** CT based on volume rendering can both simultaneously evaluate left and right cardiac function parameters in children with tetralogy of Fallot. There were no significant changes in left ventricular function parameters between the 6 months after surgery and the preoperative period, the difference was not statistically significant. Right ventricular end-systolic volume 6 months after surgery was higher than that in the preoperative period [(23.88±7.44) mL/m² vs (19.67±6.52) mL/m²], but the difference was not statistically significant ($P=0.066$). Right ventricular end-diastolic volume six months after surgery was higher than preoperative volume [(49.86±14.82) mL/m² vs (46.30±14.46) mL/m²], but the difference was not statistically significant ($P=0.079$); and the right ventricular ejection fraction was significantly lower than that before surgery (51.47%±4.68% vs 57.84%±5.09%), the difference was statistically significant ($P=0.001$). **Conclusion:** CT based on volume rendering can accurately evaluate the preoperative and postoperative left and right cardiac function in children with tetralogy of Fallot, and can detect the early decline of right cardiac function after surgery, which is important for the assessment of prognosis in children with repaired tetralogy of Fallot.

Keywords computed tomography; tetralogy of Fallot; cardiac function; threshold-based segmentation

法洛四联症(tetralogy of Fallot, TOF)是最儿童最常见的青紫型复杂性先天性心脏病(congenital heart disease, CHD)。TOF患儿术前、术后左心和右心功能进行准确评估和形态观察对提高TOF根治术的治愈率,治疗评估和判断预后具有重要指导意义^[1-3]。TOF矫治后的长期心脏合并症包括慢性肺动脉反流,右心室容量超负荷,心律失常,右心和左心室功能障碍,心室功能,尤其是右心室功能障碍进一步显示预测不良TOF预后^[4-5],因此,准确评估TOF术前与术后心功能参数,对判断儿童TOF预后具有重要意义。目前临床儿童CHD影像学诊断和评估心功能方法包括超声心动图,心脏磁共振(cardiac magnetic resonance, CMR)和CT。CMR是评估右心功能的金标准,因为其能够定量心室容积和肺动脉血流^[6-9],但是由于其检查时间较长等原因,在儿童中的应用受到较大限制。因右心室几何结构较为复杂,不如左心室规则,超声心动图评估右心功能也受到一定的限制^[6]。CT相对于CMR及超声心动图具有较高的空间分辨率和时间分辨率,在评估儿童TOF心功能罕见报道,因此本研究拟探讨基于CT阈值分割评估TOF患儿术前、术后心功能变化中的临床应用价值,旨在为儿童TOF诊疗提供参考。

1 对象与方法

1.1 对象

回顾性纳入2018年11月至2019年12月浙江大学医学院附属儿童医院确诊为TOF并行手术治疗的38例患儿,年龄3.7~30.0(11.9±5.4)个月,体重5.9~13.5(9.1±2.8) kg。纳入的患儿于手术前和手术后6个月行心脏CT扫描。纳入标准:符合TOF诊断标准;未合并其他重要畸形;术后按时随访;术前及术后随访行CTA检查。排除标准:有冠脉疾病、肺部感染、慢性肾病和患有遗传代谢疾病的患儿。

1.2 方法

1.2.1 CT扫描仪器和方法

应用美国GE公司64排螺旋CT扫描仪LightSpeed Volume CT(GE Healthcare, United States)进行检查。所有患儿通过外周静脉注射2 mL/kg非离子造影剂(碘帕醇,370 mg/mL,Bracco,意大利)。根据静脉导管的尺寸和稳定性,注射器的造影剂注射速率为0.8~2.5 mL/s。扫描范围从胸腔入口水平调整到横膈膜水平。扫描参数:CT检查均采用回顾性心电门控,螺旋采集,64个检测器的准直×0.625 mm,旋转速度0.35 s,螺距约0.2,管电压设置为100 kV,电

流150~300 mA, 用标准(STND)核重建心脏横向图像, FOV为250 mm×250 mm, 矩阵尺寸为512×512, 层厚为0.625 mm。所有图像均行多期相重建, CT原始数据传输到后处理工作站(Advantage Windows 4.2, General Electric, Milwaukee, WI, USA)进行图像分析。

1.2.2 图像后处理及心功能测定

CT图像数据根据回顾性心电门控(retrospective ECG-gating), 以5%期相为间隔, 将R-R间期分为20个期相进行重建, 重建后用DVD光盘保存为DICOM格式数据, 以心室短轴位最小及最大横径期相选取心室收缩末期、舒张末期。研究^[10]表明: 当心率 ≥ 80 次/min时, 舒张末期可选择0% R-R间期时相, 收缩末期可选择40%~45% R-R间期时相, 因此本研究选取0%为舒张末期, 选取45%为收缩末期。将图像导入Mimics 19.0软件

进行后处理, 图像数据导入后, 选取最佳阈值, 软件根据所选取的阈值生成蒙版, 生成三维图像, 根据软件CT Heart模块可分割出左、右心室(图1)结构。乳头肌和腱索未纳入血池内, 因此不计算入心室容积, 获得的心功能参数包括左室舒张末期容积(left ventricular end-diastolic volume, LVEDV)、左室收缩末期容积(left ventricular end-systolic volume, LVESV)、右室舒张末期容积(right ventricular end-diastolic volume, RVEDV)、右室收缩末期容积(right ventricular end-systolic volume, RVESV)、左室搏出量(left ventricular stroke volume, LVSV)、右室搏出量(right ventricular stroke volume, RVSV)、左室射血分数(left ventricular ejection fraction, LVEF)、右室射血分数(right ventricular ejection fraction, RVEF)。每个病例重复操作3次, 取平均值作为最后的测量结果。

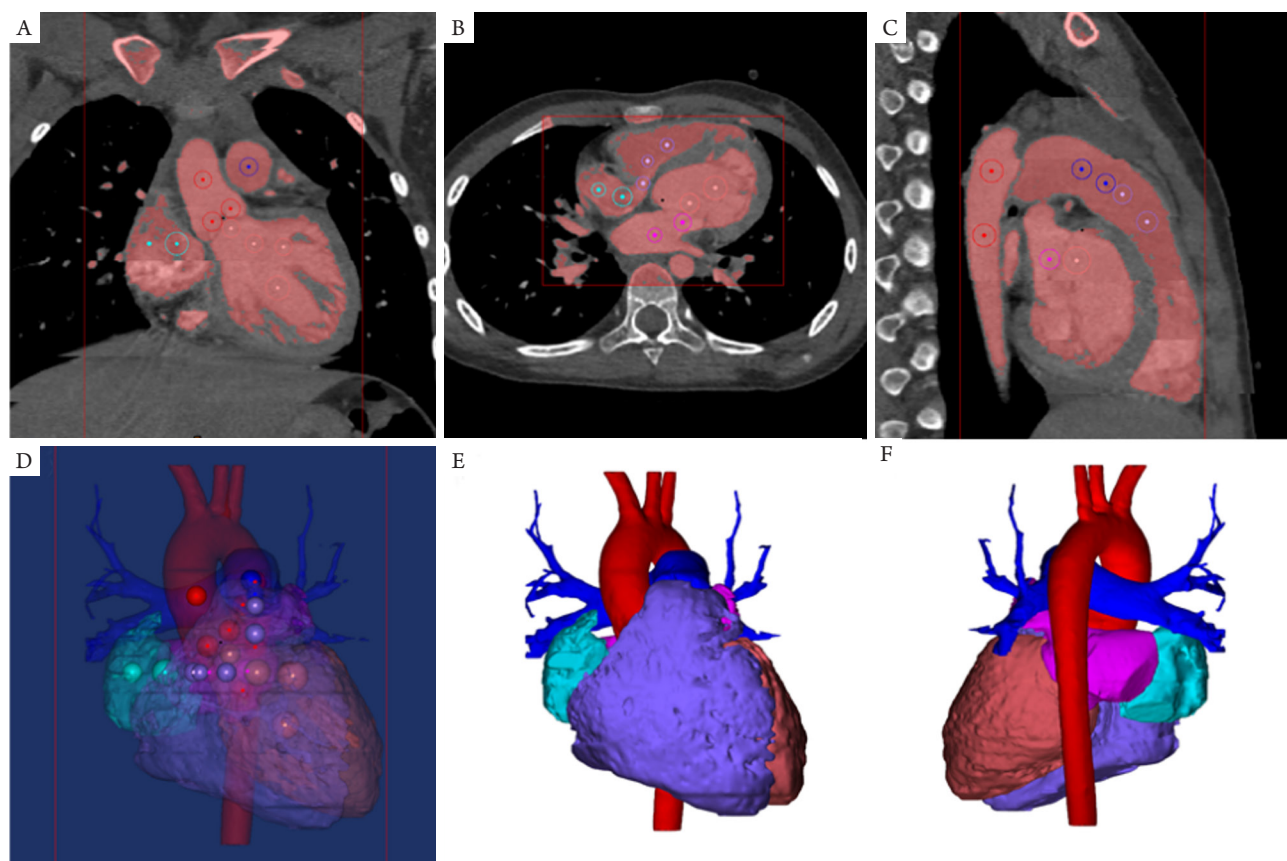


图1 三维建模流程图

Figure 1 Three-dimensional modeling flow chart

(A~C)分别为冠状面、横断面、矢状面的蒙版视图, 并对左心室(LV)、右心室(RV)、左心房(LA)、右心房(RA)、主动脉(AO)、肺动脉(PA)进行标注; (D)标注后的三维视图; (E、F)计算蒙版得到的平滑三维图像分别为前面观、后面观。

(A~C) are in the coronal, cross-sectional, and sagittal masked views, respectively and the left ventricle (LV), right ventricle (RV), left atrium (LA), and right atrium (RA), aorta (AO), and pulmonary artery (PA) are labeled; (D) the three-dimensional view is labeled; (E, F) the smooth three-dimensional images obtained by calculating the mask the front view and the back view, respectively.

1.3 统计学处理

采用SPSS 20.0统计学软件进行数据分析。符合正态分布的计量资料以均数±标准差($\bar{x}\pm s$)表示。术前、术后心功能参数符合正态分布, 差异比较采用配对 t 检验, 以 $P<0.05$ 为差异具有统计学意义。

2 结果

基于CT阈值分割可精准重建出左右心室三维结构。术前血池平均分割阈值为(212.7±20.8) HU, 心肌平均分割阈值为(93.0±10.7) HU, 左室平均分割阈值为(204.8±15.6) HU, 右室平均分割阈值为(225.9±18.3) HU, 术后血池平均分割阈值为(219.2±23.1) HU, 心肌平均分割阈值为

(94.1±9.8) HU, 左室平均分割阈值为(205.6±14.5) HU, 右室平均分割阈值为(223.8±16.6) HU。图像处理及心功能计算耗时平均约15 min, 分割出左、右心房、左、右心室舒张末期及收缩末期(图2)。TOF患儿术前及术后所测得的心功能参数见表1, 结果显示: 术后6个月与术前相比, 左心功能参数无明显变化, 差异无统计学意义($P>0.05$); 右心收缩末期容积略高于术前[(23.88±7.44) mL/m² vs (19.67±6.52) mL/m²], 但差异无统计学意义($P=0.066$), 右心室舒张末期容积略高于术前[(49.86±14.82) mL/m² vs (46.30±14.46) mL/m²], 但差异无统计学意义($P=0.079$); 右心射血分数低于术前(51.47%±4.68% vs 57.84%±5.09%), 差异有统计学意义($P=0.001$)。

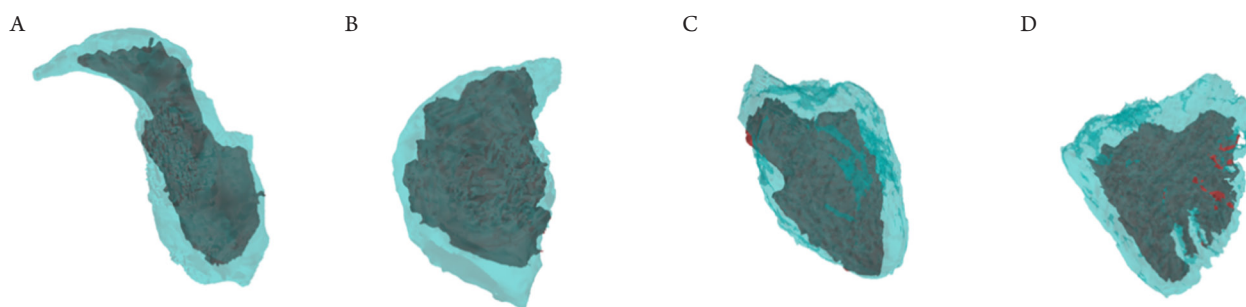


图2 阈值分割: (A、B)左心房、右心房在一个心动周期最大(浅绿色)、最小体积(灰黑色)形态对比; (C、D)左心室、右心室舒张末期(浅绿色)及收缩末期(灰黑色)形态对比

Figure 2 Threshold segmentation: (A, B) maximum (light green) and minimum volume (gray black) and morphological comparison of left atrium and right atrium in a cardiac cycle; (C, D) left ventricle, right ventricle at end-diastolic stage (light green) and end-systolic stage (gray-black)

表1 TOF术前与术后6个月左右心室功能对比($n=38$)

Table 1 Comparison of ventricular function before and 6 months after operation in TOF ($n=38$)

组别	术前	术后	t	P
LVEDV/(mL·m ⁻²)	42.40 ± 13.75	43.10 ± 13.53	0.449	0.736
LVESV/(mL·m ⁻²)	16.77 ± 5.20	17.23 ± 5.26	0.651	0.520
LVSV/(mL·m ⁻²)	25.68 ± 8.03	24.92 ± 8.98	0.568	0.680
LVEF/%	60.99 ± 4.81	59.28 ± 4.21	0.651	0.563
RVEDV/(mL·m ⁻²)	46.30 ± 14.46	49.86 ± 14.82	1.835	0.079
RVESV/(mL·m ⁻²)	19.67 ± 6.52	23.88 ± 7.44	1.960	0.066
RVSV/(mL·m ⁻²)	26.59 ± 8.25	25.74 ± 8.80	1.125	0.280
RVEF/%	57.84 ± 5.09	51.47 ± 4.68	3.891	0.001

3 讨论

TOF是最常见的青紫型CHD, 虽然经过手术治疗预后有明显改善, 但是术后远期右心功能不全的发生率仍高达38.2%^[11]。TOF患者术后会出现右心功能下降^[12-13], 且TOF术后右心功能下降与患者术后远期活动耐力降低、病死率密切相关^[14-16]。因此早期发现TOF术后右心功能的改变并积极干预, 是改善预后的重要措施, 因此对TOF患者术后右心功能评价对于干预具有重要的指导意义。

TOF患者右心功能评估是临床中较为重要的问题: 右心室由于其形状较为复杂, 并且位于胸骨后方, 内膜极为不规则, 流入道与流出道不在同一平面, 导致传统的二维超声心动图在评估右心室形态和心功能存在较大的难度, 并且超声心动图受诊断医生的主观经验水平等因素影响。CMR是目前评价心功能的金标准, 但是其检查时间长、年龄较小的婴幼儿需要较长时间镇静、价格较为昂贵、禁忌证较多等缺点限制了其在婴幼儿中的应用。近年来, CT逐渐应用于评价CHD心功能, 并且具有较高的准确性^[17]。

本研究结果显示: 应用CT评估儿童TOF心功能具有可行性, 38例行TOF手术治疗患儿与术前左心功能相比, 术后6个月左心功能无明显变化, 原因可能为手术纠正解剖畸形后, 左室收缩性能和前负荷可恢复正常, 因而在TOF术后, 左心功能往往较少降低。Ye等^[18]应用超声心动图评估了TOF患儿术前LVEF, 平均为64.34%±10.53%, 本研究中CT评估TOF患儿术前平均LVEF为60.99%±4.81%, 结果较为一致。术后6个月右心舒张末期容积及收缩末期容积均略高于术前, 虽然差异无统计学意义, 但已说明TOF术后存在右心扩大、收缩功能降低的问题, 同时术后右心射血分数明显低于术前右心射血分数, 表明术后6个月即有右心功能下降, 而此时往往无明显临床症状, 说明早期评估术后右心射血分数可先于临床症状预测右心功能下降, 本研究与邹隽麟等^[19]的研究结果一致。右心扩大原因是因为TOF矫治术后, 存在肺动脉反流, 导致右心容量负荷增加, 由于慢性容量负荷增加导致游离壁扩张及室间隔左移导致室间隔功能障碍, 右心收缩性能逐渐下降, 导致射血分数降低^[20]。因此CT可应用于TOF术后评估心功能, 早期发现右心功能下降, 指导早期采取积极干预措施改善患者生存率。CT基于阈值分割法评估CHD心室收缩末期及舒张末期容积具有较高的准确性,

CT可用于评估整个TOF术前术后期间的右心室容积, 容量负荷和心功能^[17,21-23], 可早期发现TOF术后右心射血分数降低。目前, CMR评估心功能分割方法是使用短轴位电影序列描绘心内膜边界进行计算, 然而, 这种方法将乳头肌和腱索计算在心室容积内。研究^[24-28]表明: 包含或排除乳头肌和腱索作为心室容量的一部分可能导致不同的结果, 从而对射血分数产生影响。将乳头肌和腱索计算入心室容积可导致心室容积偏高, 射血分数结果偏低。本研究将乳头肌和腱索排除于心室容积, 更接近真实值, 因为真正的心室容积不含乳头肌和腱索体积。

本研究也存在一些不足之处, 尽管心脏大血管CTA及其三维重建可清晰显示心脏大血管结构, 为外科医生手术提供更加直观和完整的解剖结构, 但是相对于心脏超声, CTA具有一定的电离辐射。本研究中38例患儿CTA平均有效辐射剂量为(0.936±0.202) mSv, 与已往研究^[29-30]结果相近。对于如TOF等复杂性CHD, CTA仍具有不可替代的作用, 为外科手术保驾护航。心脏超声对于先天性如单纯室间隔缺损、房间隔缺损诊断具有较高的准确性; 对于合并有多种畸形的复杂性CHD, CTA具有较高的准确性, 尽管其花费较心脏超声更多, 但其作用不可代替。因此在复杂性CHD的诊断中, CTA具有重要的作用, 临床应用也较为广泛。在今后的研究中, 如何进一步降低CTA对低龄儿童的辐射剂量是一个重要的问题。

综上所述, 基于CT阈值分割可准确评估TOF患儿术前、术后左、右心功能参数, 可以早期发现患儿术后右心功能下降, 从而积极采取干预措施, 对TOF患儿预后评估有重要意义, 且一次检查可同时实现心脏结构和功能的评估。

参考文献

1. van Straten A, Vliegen HW, Hazekamp MG, et al. Right ventricular function after pulmonary valve replacement in patients with tetralogy of Fallot[J]. *Radiology*, 2004, 233(3): 824-829.
2. Dragulescu A, Friedberg MK, Grosse-Wortmann L, et al. Effect of chronic right ventricular volume overload on ventricular interaction in patients after tetralogy of Fallot repair[J]. *J Am Soc Echocardiogr*, 2014, 27(8): 896-902.
3. Cai K, Rongqian Y, Li L, et al. Tetralogy of Fallot cardiac function evaluation and intelligent diagnosis based on dual-source computed tomography cardiac images[J]. *Artif Organs*, 2016, 40(5): 459-469.

4. Mohamed I, Stamm R, Keenan R, et al. Assessment of disease progression in patients with repaired tetralogy of fallot using cardiac magnetic resonance imaging: a systematic review[J]. *Heart Lung Circ*, 2020, 29(11): 1613-1620.
5. Lenoir M, Chenu C, Amrous A, et al. Right ventricular remodelling after endo-exclusion during pulmonary valve replacement: evaluation by cardiac magnetic resonance[J/OL]. *Eur J Cardiothorac Surg*, 2021, Epub ahead of print.
6. Mocerri P, Duchateau N, Gillon S, et al. Three-dimensional right ventricular shape and strain in congenital heart disease patients with right ventricular chronic volume loading[J/OL]. *Eur Heart J Cardiovasc Imaging*, 2020, Epub ahead of print.
7. Petersen SE, Aung N, Sanghvi MM, et al. Reference ranges for cardiac structure and function using cardiovascular magnetic resonance (CMR) in Caucasians from the UK Biobank population cohort[J]. *J Cardiovasc Magn Reson*, 2017, 19(1): 18.
8. Souto Bayarri M, Masip Capdevila L, Remuñan Pereira C, et al. Cardiac magnetic resonance analysis of right ventricular function: comparison of quantification in the short-axis and 4-chamber planes[J]. *Radiologia*, 2015, 57(1): 50-55.
9. Nucifora G, Sree Raman K, Muser D, et al. Cardiac magnetic resonance evaluation of left ventricular functional, morphological, and structural features in children and adolescents vs. young adults with isolated left ventricular non-compaction[J]. *Int J Cardiol*, 2017, 246: 68-73.
10. Hong SH, Goo HW, Maeda E, et al. User-friendly vendor-specific guideline for pediatric cardiothoracic computed tomography provided by the Asian society of cardiovascular imaging congenital heart disease study group: part 1. Imaging techniques[J]. *Korean J Radiol*, 2019, 20(2): 190-204.
11. Zheng DW, Shao GF, Feng Q, et al. Long-term outcome of correction of tetralogy of Fallot in 56 adult patients[J]. *Chin Med J (Engl)*, 2013, 126(19): 3675-3679.
12. Raj R, Puri GD, Jayant A, et al. Perioperative echocardiography-derived right ventricle function parameters and early outcomes after tetralogy of Fallot repair in mid-childhood: a single-center, prospective observational study[J]. *Echocardiography*, 2016, 33(11): 1710-1717.
13. Abd El Rahman MY, Hui W, Schuck R, et al. Regional analysis of longitudinal systolic function of the right ventricle after corrective surgery of tetralogy of Fallot using myocardial isovolumetric acceleration index[J]. *Pediatr Cardiol*, 2013, 34(8): 1848-1853.
14. Schäfer M, Browne LP, Jaggars J, et al. Abnormal left ventricular flow organization following repair of tetralogy of Fallot[J]. *J Thorac Cardiovasc Surg*, 2020, 160(4): 1008-1015.
15. Padalino MA, Cavalli G, Albanese SB, et al. Long-term outcomes following transatrial versus transventricular repair on right ventricular function in tetralogy of Fallot[J]. *J Card Surg*, 2017, 32(11): 712-720.
16. Friedberg MK, Fernandes FP, Roche SL, et al. Impaired right and left ventricular diastolic myocardial mechanics and filling in asymptomatic children and adolescents after repair of tetralogy of Fallot[J]. *Eur Heart J Cardiovasc Imaging*, 2012, 13(11): 905-913.
17. Goo HW. Right ventricular mass quantification using cardiac CT and a semiautomatic three-dimensional hybrid segmentation approach: a pilot study[J]. *Korean J Radiol*, 2021, 22(6): 901-911.
18. Ye JJ, Shu Q, Liu XW, et al. Noninvasive perioperative evaluation of right ventricular function in children with tetralogy of Fallot[J]. *Artif Organs*, 2014, 38(1): 41-47.
19. 邹隽麟, 孙泽琳, 张赛丹, 等. 三维超声心动图对法洛四联症患者术后右心室功能的评估[J]. *中国医学物理学杂志*, 2018, 35(10): 1145-1149.
ZOU Junlin, SUN Zelin, ZHANG Saidan, et al. Evaluation of postoperative right ventricular function in patients with tetralogy of Fallot by three-dimensional echocardiography[J]. *Chinese Journal of Medical Physics*, 2018, 35(10): 1145-1149.
20. Nair KK, Ganapathi S, Sasidharan B, et al. Asymptomatic right ventricular dysfunction in surgically repaired adult tetralogy of fallot patients[J]. *Ann Pediatr Cardiol*, 2013, 6(1): 24-28.
21. Goo HW. Comparison between three-dimensional navigator-gated whole-heart MRI and two-dimensional cine MRI in quantifying ventricular volumes[J]. *Korean J Radiol*, 2018, 19(4): 704-714.
22. Goo HW. Changes in right ventricular volume, volume load, and function measured with cardiac computed tomography over the entire time course of tetralogy of Fallot[J]. *Korean J Radiol*, 2019, 20(6): 956-966.
23. Siripornpitak S, Goo HW, et al. CT and MRI for repaired complex adult congenital heart diseases[J]. *Korean J Radiol*, 2021, 22(3): 308-323.
24. Goo HW, Park SH, et al. Semiautomatic three-dimensional CT ventricular volumetry in patients with congenital heart disease: agreement between two methods with different user interaction[J]. *Int J Cardiovasc Imaging*, 2015, 31 Suppl 2: 223-232.
25. Petitjean C, Dacher JN, et al. A review of segmentation methods in short axis cardiac MR images[J]. *Med Image Anal*, 2011, 15(2): 169-184.
26. Freling HG, van Wijk K, Jaspers K, et al. Impact of right ventricular endocardial trabeculae on volumes and function assessed by CMR in patients with tetralogy of Fallot[J]. *Int J Cardiovasc Imaging*, 2013, 29(3): 625-631.
27. Miller CA, Jordan P, Borg A, et al. Quantification of left ventricular indices from SSFP cine imaging: impact of real-world variability in analysis methodology and utility of geometric modeling[J]. *J Magn Reson Imaging*, 2013, 37(5): 1213-1222.
28. Mao SS, Li D, Rosenthal DG, et al. Dual-standard reference values of left ventricular volumetric parameters by multidetector CT angiography[J]. *J Cardiovasc Comput Tomogr*, 2013, 7(4): 234-240.

29. 张健, 杨明, 莫绪明, 等. 不同管电压64层螺旋CT对儿童CTA图像质量和辐射剂量的影响[J]. 中国医学影像技术, 2012, 28(6): 1213-1217.
ZHANG Jian, YANG Ming, MO Xuming, et al. Impact of different tube voltage protocols on image quality and radiation dosage for pediatric 64-slice cardiovascular CT angiography[J]. Chinese Journal of Medical Imaging Technology, 2012, 28(6): 1213-1217.
30. 毕璐琳, 杨辉. “双低”扫描技术在儿童先天性心血管成像中的应用[J]. 中国药物与临床, 2020, 20(22): 3721-3723.
BI Lulin, YANG Hui. Application of “double low” scanning technique in angiography of congenital heart disease in children[J]. Chinese Remedies & Clinics, 2020, 20(22): 3721-3723.

本文引用: 应波, 徐佳俊, 钱红萍. 基于计算机断层扫描阈值分割评估儿童法洛四联症心功能的临床应用价值[J]. 临床与病理杂志, 2022, 42(5): 1086-1092. doi: 10.3978/j.issn.2095-6959.2022.05.011

Cite this article as: YING Bo, XU Jiajun, QIAN Hongping. Clinical value of computed tomography based on volume rendering in assessment of cardiac function in children with tetralogy of Fallot[J]. Journal of Clinical and Pathological Research, 2022, 42(5): 1086-1092. doi: 10.3978/j.issn.2095-6959.2022.05.011